

SURFACE FUNCTIONALIZATION OF QUARTZ FIBRES BY DIRECT GROWTH OF CARBON NANOSTRUCTURES

Ginevra, Lalle^a, Matteo, Lilli^a, Luiz H., Acauan^b, Brian L., Wardle^{b,c}, Ilaria, Rago^{d,e}, Gianluca, Cavoto^{d,e}, Francesco, Pandolfi^e, Fabrizio, Sarasini^a, Jacopo, Tirillò^a

a: Department of Chemical Engineering Materials Environment, Sapienza-Università di Roma, Via Eudossiana 18, 00184, Roma, Italy– ginevra.lalle@uniroma1.it

b: Department of Aeronautics and Astronautics, Massachusetts Institute of Technology, 77 Massachusetts Ave., Cambridge, MA, 02139, USA

c: Department of Mechanical Engineering, Massachusetts Institute of Technology, 77 Massachusetts Ave., Cambridge, MA, 02139, USA

d: Dipartimento di Fisica 'Sapienza' Università di Roma and INFN Sezione di Roma, Piazzale Aldo Moro 2, 00185, Rome, Italy

e: INFN Sezione di Roma, Piazzale Aldo Moro 2, 00185, Rome, Italy

Abstract: *The aim of the present work is to investigate the direct growth of carbon nanostructures (CNSs) onto quartz fibres to improve interfacial properties in polymer composites. Mechanical properties of quartz fibres are known to be reduced due to exposure to typical conditions (primarily temperature) for CNS growth, e.g., herein quartz fibres at 600 °C for 1h in air give a strength loss of 58%. Cu as a novel low-temperature (<500 °C) catalyst is explored as an alternative to the more typical Fe which requires temperatures higher than 600 °C. As part of a larger study, Cu- and Fe-catalysed CNS growth on quartz fibres are shown at high temperature (740 °C). Weibull analysis of the tensile data, FE-SEM investigation and X-ray diffraction analysis were carried out to identify possible damage mechanisms in the exemplary heat-treated fibres, setting up additional work to compare results at lower-temperature CNS growth known to be achievable with copper.*

Keywords: Quartz fibres; Chemical vapour deposition (CVD); Carbon nanostructures; Interface/Interphase

1. Introduction

Grafting carbon nanostructures (CNSs) onto the surface of microscale reinforcing fibres improves the structural performance of fibre-reinforced polymers (FRPs) by enhancing fibre/matrix interfacial adhesion and matrix-dominated properties [1]. Moreover, due to the unique properties of CNSs, their incorporation into composite materials offers the opportunity to implement additional electrical, chemical, or thermal functions.

Among the techniques reported to graft CNSs onto the fibre surface, direct growth through chemical vapour deposition (CVD) is often preferred as it ensures excellent control over the density and orientation of CNSs [2]. Direct CNS growth has been explored on various fibre materials, including carbon, glass, and alumina fibres. However, depending on the substrate, the high temperatures involved in the CVD process (≥ 600 °C) may have detrimental effects on the mechanical properties of the fibres. The most severe thermal degradation is observed in the case of E-glass fibres, which exhibit appreciable strength losses at temperatures as low as 250 °C [3]. Quartz fibres, also known as ultrapure silica glass fibres, are designed to withstand service temperatures much higher than E- or S-glass fibres. Therefore, they are emerging as a promising

candidate for the direct growth of CNSs. Recently, De Luca et al. [4] achieved uniform coverage of carbon nanotubes (CNTs) on quartz fibres resulting in both a 12% improvement of IFSS and a piezo-resistive response suitable for strain-sensing applications. Nevertheless, they detected a 50% decrease of the tensile strength of the fibres exposed to 760 °C for 30 minutes in N₂. A significant drop of quartz fibre tensile strength was also reported by Zheng et al. [5] after 10-hour exposure in the temperature range 600-900 °C in air atmosphere. However, whilst the thermal strength loss of general-purpose glass fibres has been widely investigated, mechanisms behind quartz fibre strength loss still need to be clarified.

To preserve the mechanical properties of the pristine fibres, a new catalyst, namely copper, can be employed to reduce CNS growth temperature, as it requires lower temperatures to be activated (<500 °C) [6] than the more common catalysts based on Fe, Ni and Co. This work is part of a larger study aiming at (i) assessing the effects of thermal exposure to medium-high temperatures (400-800 °C) on the mechanical properties of quartz fibres and discussing the resulting damage modes, and (ii) achieving low-temperature CVD growth of CNSs on quartz fibres using Cu as an innovative catalyst. In particular, this paper discusses at first the behaviour of quartz fibres exposed for 1h at 600 °C in air as a benchmark for highlighting the decrease in mechanical properties and then reports on Cu- and Fe-catalysed CNS growth at high temperature (740 °C), as a preliminary research aimed at achieving lower-temperature CNS growth by means of future optimization of the process parameters. It is worth noting that thermal exposure in air usually represents the worst scenario for fibre degradation compared to inert atmospheres [3].

2. Materials and methods

2.1 Raw materials

Quartz fibres (Quartzel® C14 1600 QS1318) with a commercial epoxy resin compatible sizing were kindly provided by Saint-Gobain as a continuous roving with a nominal fibre diameter of 14 µm. Catalyst precursors for the CVD process were iron (III) nitrate nonahydrate (Fe(NO₃)₃·9H₂O, ≥98%) and copper(II) acetate monohydrate (Cu(CH₃COO)₂·H₂O, ≥98%). Such precursors were dissolved in 2-propanol ((CH₃)₂CHOH, ≥99.5%) and acetonitrile (C₂H₃N, ≥99%), respectively.

2.2 Mechanical characterization of single fibres

A tube furnace (Lenton Thermal Designs Ltd., Hope, UK) was used to heat treat bundles of as-received quartz fibres at 600 °C for 1 hour in air atmosphere. Cooling of the fibres was carried out outside the furnace at room temperature. After the heat treatment, tensile tests were conducted at room temperature on both as-received and heat-treated fibres. Tests were carried out in accordance with ASTM C1557, using a Zwick/Roell Z010 tensile machine equipped with a 100 N range load cell. Displacement control and a cross-head speed of 2 mm/min were selected. At least 60 specimens with a gauge length of 20 mm were tested for each group of fibres. The actual specimen elongation was calculated by subtracting the displacement related to the system compliance from the total cross-head displacement. To evaluate the system compliance, specimens of as-received fibres were tested at three different gauge lengths, i.e., 20 mm, 30 mm, and 40 mm.

The data of the tensile strength and Young's modulus were analysed using the two parameter Weibull distribution in equation (1)

$$F(\sigma) = 1 - \exp \left[- \left(\frac{\sigma}{\sigma_0} \right)^m \right] \quad (1)$$

where $F(\sigma)$ is the probability of failure at a stress σ , m is the Weibull modulus and σ_0 is a scale parameter. The probability of failure was estimated according to equation (2):

$$F_j = \frac{j-0.5}{N} \quad (2)$$

where N is the number of tested specimens and j is the rank of the j th data point.

2.3 Growth procedure of carbon nanostructures

Prior to the CVD growth, catalyst precursors were deposited onto the surface of quartz fibres by dip-coating. To achieve the deposition of a Fe-based catalyst precursor, bundles of as-received fibres were dipped into a 50 mM solution of iron(III) nitrate nonahydrate in 2-propanol for 5 minutes. The Cu-based precursor was deposited by dipping into a solution of copper(II) acetate monohydrate in acetonitrile. The molarities (1, 2.5 and 5 mM) and the immersion times (3, 4.5 and 6 h) were varied to find the optimal conditions for uniform CNS growth onto the fibre surface. Both processes were carried out at room temperature. After the deposition process, fibres were allowed to dry at room temperature overnight.

Subsequently, catalyst-solution coated quartz fibres were located on the heating element of a high vacuum reaction chamber to achieve the growth of CNSs through Fe- and Cu-catalysed CVD. To reduce the catalyst precursor and achieve a homogeneous distribution of active nanoparticles on the fibre surface, an annealing treatment was first performed. H₂ was introduced into the chamber up to a partial pressure of 8·10⁻¹ mbar and temperature was raised at 720 °C for 4 minutes. Afterwards, the actual growth process was carried out at 740 °C for 10 minutes by introducing acetylene as a carbon source up to a partial pressure of 60–70 mbar. Finally, the fibres were allowed to cool down to room temperature.

2.4 Morphological and structural characterizations

Morphological investigations of lateral and fracture surfaces of the fibres were carried out by means of a Mira3 field emission scanning electron microscope (FE-SEM) by Tescan. To investigate the effects of high temperature exposure on quartz fibre structure, X-ray diffraction analysis (XRD) was carried out at room temperature on as-received and heat-treated fibres by means of a Philips X'Pert PRO powder diffractometer (Cu_{K1} α radiation = 1.54060 Å, Cu_{K2} α radiation = 1.54443 Å). XRD patterns were collected in the range of 2θ = 10°–70° with a scan rate of 1°/min and a scan step 2θ = 0.02°.

3. Results and Discussion

3.1 Effects of heat treatment on the mechanical properties of quartz fibres

To evaluate the consequences of exposure to typical CVD temperatures on the tensile behaviour of quartz fibres, a heat-treatment at 600 °C for 1 hour in air atmosphere was performed. Afterwards, the tensile strength and Young's modulus of untreated and heat-treated fibres were determined at room temperature by single fibre tensile tests. The results, summarized in Table 1, revealed a strength loss of ~58% for heat-treated fibres, while Young's modulus did not undergo significant changes, in accordance with a recent work on quartz fibres [4].

Table 1: Results of tensile tests for as-received (R.T.) and heat-treated single quartz fibres in terms of average value (standard deviation).

Heat-treatment temperature [°C]	Tensile strength [MPa]	Young's modulus [GPa]
R.T.	2379.1 (355.4)	89.0 (3.3)
600	1002.1 (194.9)	84.1 (5.2)

A FE-SEM investigation of the fibre fracture surfaces (Fig. 1) revealed a failure mechanism typical of brittle materials, with a characteristic morphology composed of three different regions, namely mirror, mist, and hackle, originated by changes in the crack propagation rate during breakage. The fracture mechanism did not change for heat-treated fibres, but the size of the mirror zone was found to increase, in accordance with previous works on other ceramic fibres [3,7]. For both untreated and heat-treated fibres, the location of the mirror zone indicated that the flaws responsible for failure were located on the fibre surface.

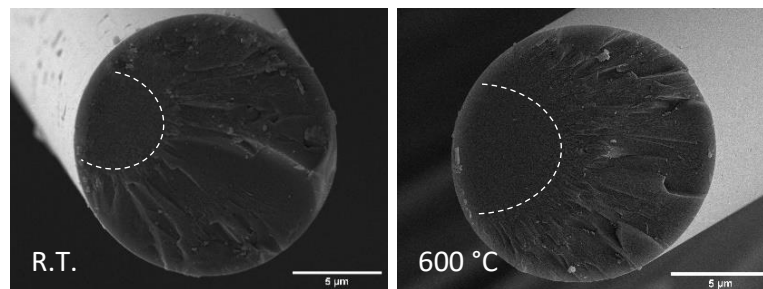


Figure 1. SEM micrographs of the fracture surfaces of as-received (R.T.) and heat treated (600 °C) quartz fibres. The mirror zone is highlighted with a white dashed line.

The outcomes from the tensile tests were analysed through a two-parameter Weibull distribution, obtaining the results reported in Table 2. The linear trend in the Weibull graph in Fig. 2 suggests the existence of a single population of defects and seems to indicate that thermal exposure does not affect the nature of defects, but rather their concentration and severity.

Table 2: Weibull distribution parameters for as-received (R.T.) and heat-treated quartz fibres.

Temperature [°C]	Tensile strength		Young's modulus	
	m_{σ}	σ_0 [MPa]	m_E	E_0 [GPa]
R.T.	8.0	2526.4	31.1	90.5
600	5.9	1082.7	19.5	86.4

As a confirmation, a morphological characterization of the fibre lateral surfaces (Fig. 3) revealed that, after heat treatment, the smooth morphology observed for as-received quartz fibres is replaced by a more irregular one. This can be ascribed to the total, or at least partial, loss of the protective sizing, which caused the exposure of the inherent fibre flaws, as previously reported

for glass fibres [8]. It is also worth noting that sizing removal directly implies a loss in the fibre/matrix interfacial adhesion of the composite material [9].

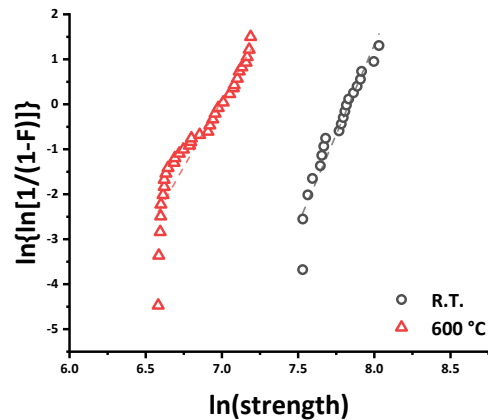


Figure 2. Weibull plot of fibre strength for as-received (R.T.) and heat treated (600 °C) quartz fibres.

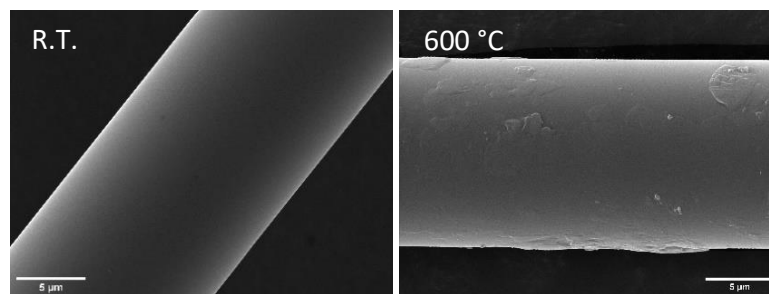


Figure 3. SEM micrographs detailing the lateral surface of as-received (R.T.) and heat treated (600 °C) quartz fibres.

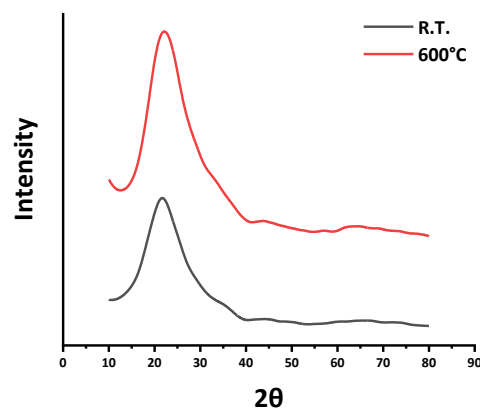


Figure 4. X-ray diffraction patterns for as-received (R.T.) and heat treated (800 °C) quartz fibres.

According to the XRD spectra reported in Fig. 4, the thermal exposure of quartz fibres did not involve crystallization phenomena, as a fully amorphous structure was identified for both as-received and heat-treated quartz fibres.

In the current study, a strength reduction mechanism that occurs predominantly at the surface of quartz fibres was identified. This is consistent with the obtained XRD spectra, which revealed no bulk structural rearrangement. The measured Young's modulus, which was hardly affected

by the heat treatment, confirms the irrelevance of any bulk modification phenomena. On the contrary, Young's modulus has been found to increase for other ceramic fibres, especially general-purpose glass fibres and basalt fibres, due to structural relaxation mechanisms occurring in the bulk of the fibres.

However, it is worth noting that structural relaxation is a phenomenon that occurs faster at the surface than in the bulk of the fibre, as previously reported by Feih et al. [3] for E-glass fibres and demonstrated by Lilli et al. [7] for basalt fibres. Therefore, due to the high drawing stress during quartz fibre fabrication, the occurrence of surface relaxation phenomena cannot be excluded, but detailed investigations are needed.

3.2 CVD growth of carbon nanostructures on quartz fibres

As a baseline for the CVD growth of CNSs onto quartz fibres, a Fe-catalysed CVD process was performed. Highly dense arrays of vertically aligned CNSs were obtained (Fig. 5). CNS diameter was around 40 nm while the length of longer CNS arrays fluctuated from 15 to 80 μm . The organization of CNSs onto the fibre surface followed a 'Mohawk' morphology, previously observed for CNSs grown on other fibres [10]. In fact, when CNS length is larger than the fibre diameter, the radial symmetry is broken and CNSs continue to grow in a common direction due to van der Waals interactions among nearby CNSs.

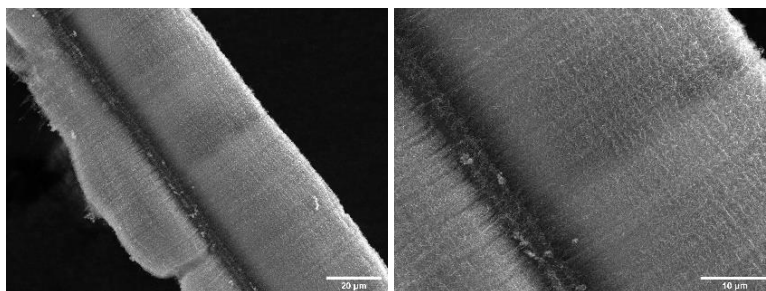


Figure 5. SEM micrographs of CNS-grafted quartz fibres following the Fe-catalysed CVD process.

Temperatures above 700 °C were necessary to achieve the Fe-catalysed growth of carbon nanostructures, in accordance with temperatures usually reported for Fe-catalysed thermal CVD [11,12]. Therefore, to meet the need for a low temperature process, Cu-catalysed thermal CVD growth of CNSs was investigated. Although copper was initially thought to be inactive towards CNS growth, in the last decade many works have demonstrated Cu-catalysed CVD growth of different CNSs, including multi-wall and single-wall CNTs [13,14]. Copper's activity towards the growth of carbon nanofibres has been proved at temperature as low as 250 °C [6], making it a promising option for low temperature CVD.

To assess the possibility to grow CNSs onto quartz fibres using Cu as a catalyst, CVD conditions were left unchanged from those previously found to be effective for Fe-catalysed growth. On the other hand, catalyst deposition conditions were varied in terms of immersion time and concentration of copper(II) acetate monohydrate in acetonitrile. A uniform growth of CNSs was achieved for fibres dipped in a 5 mM solution for 4.5 hours (Fig. 6), confirming the activity of Cu towards CNS growth. Cu-catalysed CVD led to a tangled CNS morphology with a CNS carpet thickness ranging from 2 to 8 μm . Moreover, the obtained CNSs have bigger diameters (~ 80 nm or more) than those catalysed by Fe.

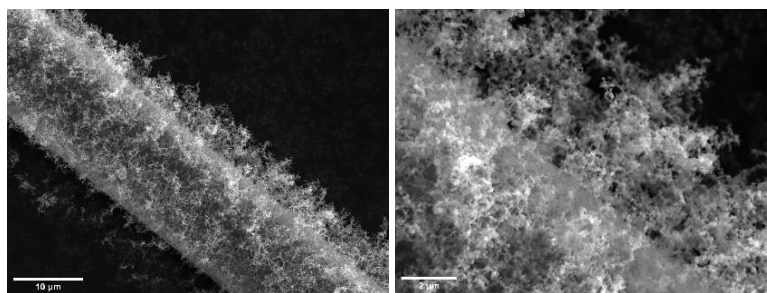


Figure 6. SEM micrographs of CNS-grafted quartz fibres following the Cu-catalysed CVD process.

4. Conclusions

The present work investigates quartz fibres as a candidate substrate for the direct growth of CNSs. The exposure to a typical CVD temperature (600 °C) for 1 hour in air atmosphere caused the strength of quartz fibres to decrease by ~58%, while no significant changes were detected for Young's modulus. These findings confirmed the higher thermal resistance of quartz fibres compared to E-glass fibres, for which strength losses of more than ~70% have been reported [8]. On the other hand, they highlighted a significant strength decay, which has been ascribed to damage mechanisms occurring at the fibre surface. To preserve the fibre mechanical properties, a first step towards the development of a low temperature growth has been taken by using an innovative catalyst, namely copper. By varying dip-coating parameters (i.e., immersion time and concentration), optimal catalyst deposition conditions were identified. A Cu-catalysed CNS growth was successfully achieved for fibres dip-coated for 4.5 hours in a 5 mM solution, using the same CVD conditions previously proved to be effective for a Fe-catalysed growth. While the Fe-catalysed CVD led to the growth of dense arrays of aligned CNSs, a tangled morphology of CNSs with bigger diameters was obtained following the Cu-catalysed process. Future work will optimize the CVD parameters of the Cu-catalysed process to control the diameter, density, and orientation of CNSs and achieve a low temperature growth.

Acknowledgements

Luiz H. Acauan and Brian L. Wardle would like to acknowledge Airbus, ANSYS, Boeing, Embraer, Lockheed Martin, Saab AB, and Teijin Carbon America through MIT's Nano-Engineered Composite aerospace Structures (NECST) Consortium.

5. References

1. Qian H, Greenhalgh ES, Shaffer MSP, Bismarck A. Carbon nanotube-based hierarchical composites: A review. *Journal of Materials Chemistry* 2010; 20(23):4751–62.
2. Sharma P, Pavelyev V, Kumar S, Mishra P, Islam SS, Tripathi N. Analysis on the synthesis of vertically aligned carbon nanotubes: growth mechanism and techniques. *Journal of Materials Science: Materials in Electronics* 2020; 31:4399–4443.
3. Feih S, Boiocchi E, Mathys G, Mathys Z, Gibson AG, Mouritz AP. Mechanical

- properties of thermally-treated and recycled glass fibres. *Composites Part B Engineering* 2011; 42(3):350–8.
4. De Luca HG, Anthony DB, Greenhalgh ES, Bismarck A, Shaffer MSP. Piezoresistive structural composites reinforced by carbon nanotube-grafted quartz fibres. *Composites Science and Technology* 2020; 198: 108275.
 5. Zheng Y, Wang S. Effect of moderately high temperature heat treatment on surface morphology and structure of quartz fibers. *Applied Surface Science* 2012; 258(10): 4698–701.
 6. Acauan LH, Kaiser AL, Wardle BL. Direct synthesis of carbon nanomaterials via surface activation of bulk copper. *Carbon* 2021; 177:1–10.
 7. Lilli M, Rossi E, Tirillò J, Sarasini F, Di Fausto L, Valente T, et al. Quantitative multi-scale characterization of single basalt fibres: Insights into strength loss mechanisms after thermal conditioning. *Material Science & Engineering A* 2020; 797:139963.
 8. Thomason JL, Yang L, Meier R. The properties of glass fibres after conditioning at composite recycling temperatures. *Composites Part A: Applied Science and Manufacturing* 2014; 61:201–8.
 9. Thomason JL, Nagel U, Yang L, Bryce D. A study of the thermal degradation of glass fibre sizings at composite processing temperatures. *Composites Part A: Applied Science and Manufacturing* 2019; 121:56–63.
 10. Yamamoto N, John Hart A, Garcia EJ, Wicks SS, Duong HM, Slocum AH, et al. High-yield growth and morphology control of aligned carbon nanotubes on ceramic fibers for multifunctional enhancement of structural composites. *Carbon* 2009; 47(3):551–60.
 11. Rago I, Rauti R, Bevilacqua M, Calaresu I, Pozzato A, Cibinel M, et al. Carbon Nanotubes, Directly Grown on Supporting Surfaces, Improve Neuronal Activity in Hippocampal Neuronal Networks. *Advanced Biosystems* 2019; 3(5):1800286.
 12. Ulloa Severino L, Perissinotto F, Rago I, Goldoni A, Santoro R, Pesce M, Casalis L, Scaini D, Carbon nanotubes substrates alleviate pro-calcific evolution in porcine valve interstitial cells. *Nanomaterials (Basel)* 2021; 11(10): 2724-44.
 13. Hsiao CH, Lin JH. Growth of a superhydrophobic multi-walled carbon nanotube forest on quartz using flow-vapor-deposited copper catalysts. *Carbon* 2017; 124:637–41.
 14. Takagi D, Homma Y, Hibino H, Suzuki S, Kobayashi Y. Single-walled carbon nanotube growth from highly activated metal nanoparticles. *Nano Lett* 2006;6(12):2642–5.